Controlled Synthesis of α-Allenic Ester and Spiro Ketone Derivatives from Tailored α-Substituted Cycloalkanones Through Cascade Reactions: Exploring the Possible Reaction Pathways by Means of Semiempirical MO Calculations

Antonio J. Mota,[a] Aurélie Klein,[b] Florence Wendling,[b] Alain Dedieu,[a] and Michel Miesch*[b]

Keywords: Cascade reactions / Allenic esters / Spiro compounds / Semiempirical calculations / Transition states / HF catalysis

Functionalized bicyclic electrophilic allenes and (or) spiro ketones have been obtained through a cascade reaction when acetylenic ω-keto esters were treated with tetra-*n*-butylammonium fluoride (TBAF). The isolated products can be modulated by using different starting materials (i.e. varying ring size, spacer length) and reaction times. The results indicate that these reactions take place under kinetic control. In line with this, a semiempirical study was carried out in order to determine the preferred reaction pathways and the preferred *cis*/*trans* conformation of the bicyclic allenic derivatives. An excellent correlation was found between theoretical and experimental results, and the whole process dramatically depends on the presence of the HF molecule.

Introduction

Cascade reactions may be defined as multi-reaction, "one-pot" sequences in which the first reaction creates the functionality required to trigger the second one without a need to change the reaction conditions. The performance of an entire sequence of bond-forming reactions in one step requires minimal effort for the isolation, purification, and characterization of intermediate products, therefore making the entire synthetic process economically and ecologically more favorable. From the standpoint of efficiency, cascade reactions are valuable, and are highly prized if they have broad scope and occur under mild conditions. They offer a very efficient approach to the formation of multiple bonds and can therefore produce polycyclic structures in a controlled fashion, thus leading to complex target molecules, mainly natural products, that are difficult or impossible to prepare by other means.[1] This has led to the idea that chemical groups that are considered unreactive under normal conditions may react when a reactive intermediate is generated in their vicinity.

In this context, we have previously shown that acetylenic ω-keto esters are readily available compounds that undergo cascade reactions to give electrophilic allenes,[2] spiro ketones, or oxetane derivatives when treated with different bases.[3] However, in spite of the synthetic utility of these systems, to the best of our knowledge, only a few reports deal with the intramolecular reactivity of acetylenic ω-keto esters. For example, Deslongchamps and co-workers reported that polycyclic compounds could be readily obtained through the intramolecular Michael addition of cyclic β-keto esters onto conjugated acetylenic ketones.[4] More recently, Christoffers and Oertling achieved a seven-membered ring annulation through an intramolecular Michael reaction catalyzed by $FeCl_3$.[5] Nevertheless, olefinic ω-keto esters have been reported to have different intramolecular reactivities to those determined by our own methodology. For example Fukumoto and co-workers, and later Ihara and co-workers, have shown that a tandem Michael–aldol reaction took place when olefinic ω-keto esters were treated with either TBDMSOTf/NEt_3 or TMSI/$(TMS)_2NH$.[6] On the other hand, Chiu et al. reported that olefinic ω-keto esters undergo tandem conjugate reduction–aldol cyclization reactions (using Stryker's reagent) to readily afford β-hydroxyketones in good yields.[7] We now wish to report a detailed investigation of the reactivities of acetylenic ω-keto esters towards TBAF. We shall focus our attention on mechanistic considerations by means of semiempirical MO calculations.

Semiempirical MO methods suffer certain well-known problems, such as the description of the hydrogen bond (es-

[a] Laboratoire de Chimie Quantique et de Modélisation Moléculaire,
UMR 7551 CNRS/ULP, Université Louis Pasteur,
Strasbourg. 4, rue Blaise Pascal, 67000 Strasbourg, France
[b] Laboratoire de Chimie Organique Synthétique,
UMR 7123 CNRS/ULP, Université Louis Pasteur,
Strasbourg 1, rue Blaise Pascal, 67000 Strasbourg, France
Fax: +33-3-90241754
E-mail: miesch@chimie.u-strasbg.fr
Supporting information for this article is available on the WWW under http://www.eurjoc.org or from the author.

pecially problematic in MNDO), typical organic hypervalent atoms (i.e. sulfur or phosphorus), transition metals, transition states, or molecules that contain atoms for which good parametrization does not exist, or simply, for which these parameters are not available.[8] Nevertheless, these methods can quickly offer qualitative information about the atomic organization and electronic distribution of experimentally studied systems. For this reason, semiempirical methods have become very useful tools in organic chemistry. In spite of the problems associated with the use of these methods in theoretical calculations, they have been widely employed,[9] even in the description of very complex reaction mechanisms.[10]

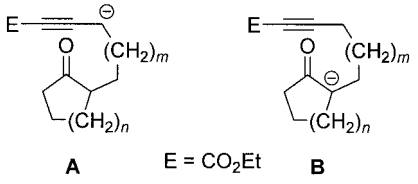

Scheme 1.

The theoretical contribution presented in this work consists of a semiempirical MO study of the potential energy space of an ensemble of propargylic (**A**) and enolate (**B**) carbanions (Scheme 1). The evolution of allenic or spiro derivatives, as well as the stereochemistry of the compounds formed, will be discussed. For this purpose, the AM1 and PM3 methods implemented in the Hyperchem 7.5 package (see Expt. Sect. for computational details) were utilized.[11]

Results and Discussion

The acetylenic ω-keto esters **1**–**4** were synthesized starting from the corresponding *N*,*N*-dimethylhydrazones using our previously developed reaction sequence (Scheme 2).[3b]

We decided to study in detail the reactivity of these compounds towards tetra-*n*-butylammonium fluoride (TBAF), whose behavior as a relatively strong base is well-documented.[12] First, we observed that no reaction took place when TBAF was used in a catalytic amount. In order to promote reaction, the use of stoichiometric quantities of TBAF proved necessary. Reactions were performed at room temperature (ca. 25 °C) and the reaction time was modified for each experiment in order to gain valuable information about the reaction kinetics.

Starting from the acetylenic ω-keto ester **1**, we noticed that the spiro derivative **5** (as a mixture of **5a**, **5b**, and **5c** isomers) was formed as the main compound. Compound **6** was formed from **5** by increasing the reaction time (Table 1).

Despite the high percentage of starting material **1** recovered after 5 min (Entry 1), this was the optimal reaction time for the production of spiro derivative **5**. Nevertheless, if our target is to obtain the polyfunctionalized ester **6**, the reaction time must be increased. Thus, after 48 h (Entry 4), compound **6** was isolated as the main product (ca. 50% yield) and results from the addition of a water molecule onto the carbonyl group, followed by a ring-opening reaction (Scheme 3).

When the length of the spacer between the cyclopentanone moiety and the electrophilic triple bond was increased by one carbon–carbon bond, the spiro derivative **7** (a mixture of the **7a**, **7b**, and **7c** isomers) and the bicyclic allene **8** [a mixture of **8a** and **8b** isomers with a *cis* ring junction as ascertained by NMR spectroscopy (NOESY experiments)] [3a] were formed as the major products. These compounds were isolated in approximately the same ratio when the reaction time was increased from 5 to 30 min (Table 2).

This means that there is no interconversion between these spirocyclic and allenic forms. However, by increasing the reaction time, allenic derivative **8** was completely transformed into the β-keto ester **9**. The latter probably results from the intramolecular addition of the corresponding alkoxide onto the central carbon of the electrophilic allene, affording a highly strained oxete ring, which evolves through a ring-opening process to give the β-keto ester **9** (Scheme 4).

By replacing the cyclopentanone ring by a cyclohexanone ring in the starting acetylenic ω-keto ester (compounds **3** and **4**), we observed that either the allene derivative **10** (mixture of isomers **10a** and **10b**) was formed as the major product along with the spiro derivatives **11**, or the unique compound **12**, depending on the length of the spacer (*m* value) (Table 3).

Note that the *cis* or *trans* diastereoselectivity observed in the formation of the bicyclic allenes **10** and **12** depends on the *m* value. The structures of these compounds were unambiguously secured by X-ray diffraction.[13]

In summary, the reactions of the acetylenic ω-keto esters **1**–**4** with TBAF generated two major products: spiro compounds **5**, **7**, and **11**, and allene compounds **8**, **10**, and **12**. Compounds **6** and **9** result from a subsequent transformation of the initial "primary" adducts, that is, of the spiro and allene derivatives, respectively (Scheme 3 and

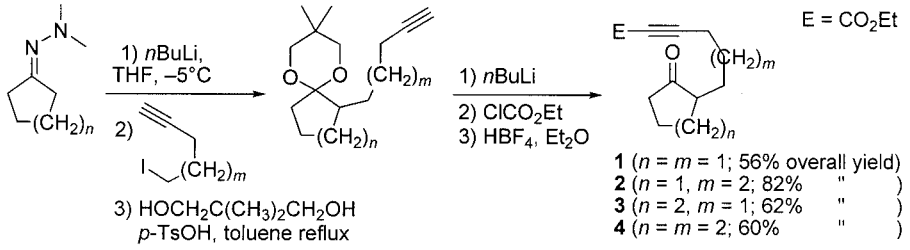

Scheme 2.

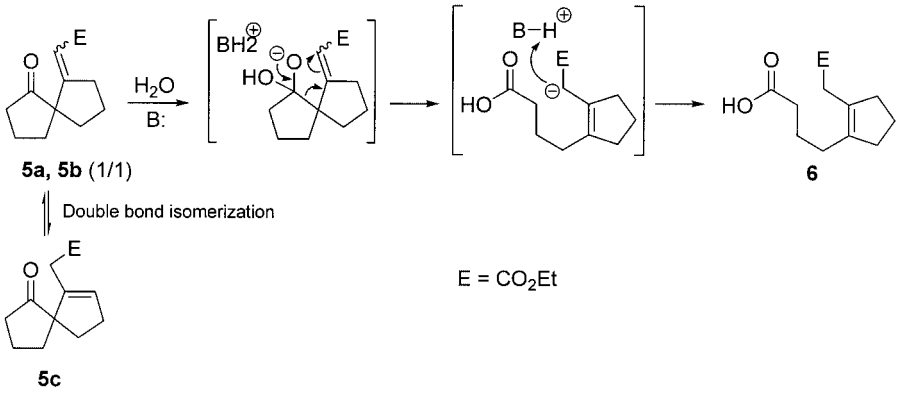

Scheme 3.

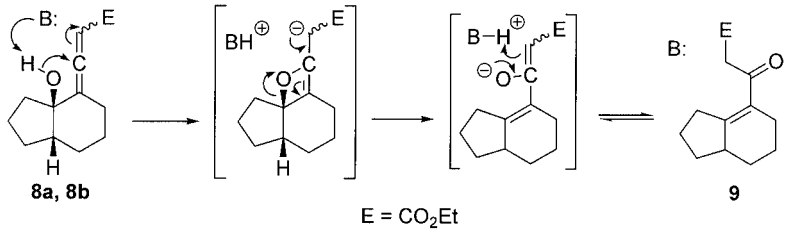

Scheme 4.

Table 1. Reaction of acetylenic ω-keto ester **1** with TBAF.

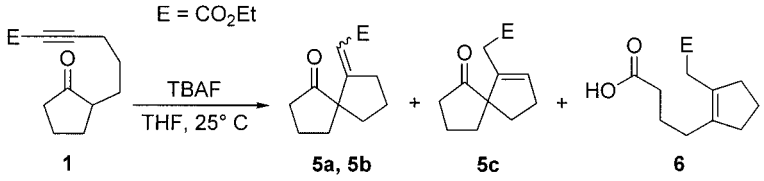

Entry	Reaction time	Yield of **5a**, **5b**, and **5c** [%][a]	Yield of **6** [%]	Yield of **1** [%][b]
1	5 min	56	–	39
2	30 min	45	8	–
3	3 h 30 min	39	36	–
4	48 h	22	49	–

[a] The **5a**, **5b**, and **5c** ratio (1:0.5:0.36) was only determined after 30 min. [b] Recovered starting material.

Table 2. Reaction of acetylenic ω-keto ester **2** with TBAF.

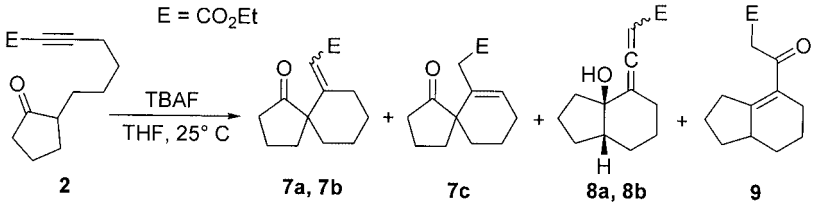

Entry	Reaction time	Yield of **7a**, **7b**, and **7c** [%][a]	Yield of **8a** and **8b** [%]	Yield of other [%]
1	5 min	40	35	7[b]
2	30 min	55	43	–
3	3 h 30 min	30	–	44[c]
4	48 h[d]	–	–	–

[a] The **7a**, **7b**, and **7c** ratio (1:0.14:0.06) was only determined after 30 min. [b] Recovered starting material (**2**). [c] Compound **9** (Scheme 4). [d] Decomposition occurred.

Table 3. Reaction of acetylenic ω-keto esters **3** and **4** with TBAF.

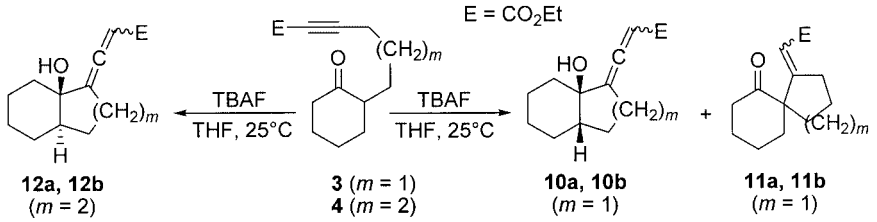

m value	Reaction time	Yield of **10a** + **10b** [%]	Yield of **11a** + **11b** [%]	Yield of **12a** + **12b** [%]	Yield of other [%]
1	5 min	45	15	–	25[a]
	30 min	59	15	–	–
	4 h[b]	–	–	–	–
2	5 min	–	–	50	50[c]
	30 min	–	–	70	20[c]
	4 h	–	–	45	20[c]

[a] Recovered starting material **3**. [b] Decomposition occurred. [c] Recovered starting material **4**.

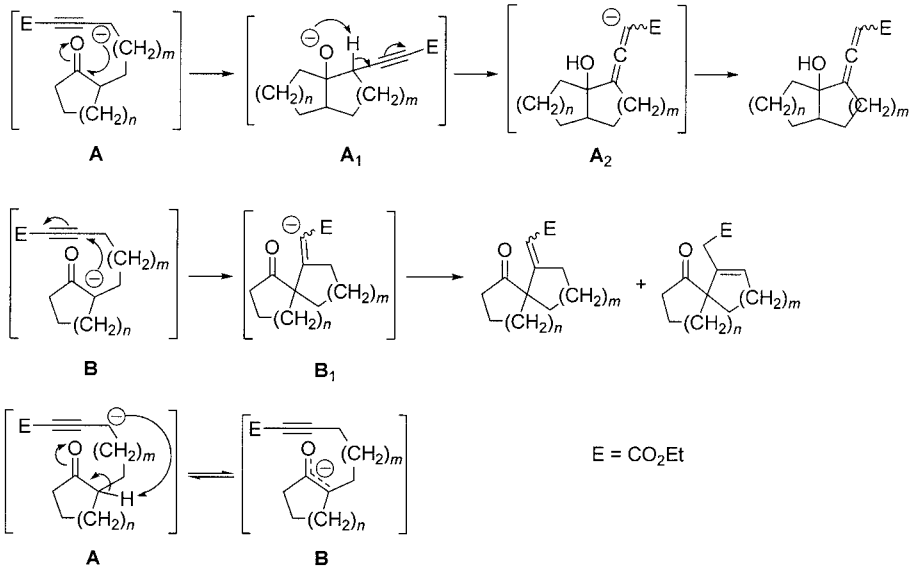

Scheme 5.

Scheme 4). Thus, TBAF can remove either one of two protons. 1) A propargylic proton leading to carbanion **A** which undergoes intramolecular addition onto the carbonyl carbon to give the alkoxide $\mathbf{A_1}$. The allene derivatives **8**, **10**, and **12** were then isolated by prototropy $\mathbf{A_1} \rightarrow \mathbf{A_2}$ (upper line in Scheme 5). 2) A hydrogen atom located in the position α to the carbonyl group in order to give carbanion **B**, which evolves through an intramolecular Michael-type addition to afford the spiro derivatives **5**, **7**, and **11** (middle line in Scheme 5).

Of course, an intramolecular process could also be involved. For instance, carbanion **B** could result directly from carbanion **A** by intramolecular hydrogen transfer or vice versa (lower line in Scheme 5).

Thus, it seems quite clear that the structures of the products obtained depend on the cycloalkanone ring size (*n* value), the length of the spacer (*m* value), and the reaction time. By combining these variables, we can synthesize a relatively wide range of new polyfunctionalized bicyclic compounds (Scheme 6).

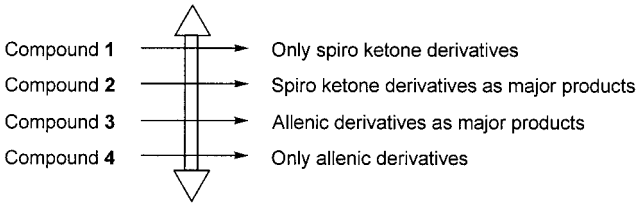

Scheme 6.

Moreover, due to the fact that the structures of interest were formed within only five minutes, and taking into account the fact that only allenic or spiro structures were generated in situ, we can conclude that i. the reaction takes place under kinetic control, ii. the two kinds of products (allenic or spiro derivatives) are not interconvertible, that

is, the $\mathbf{A_1}$ &rlhar2 $\mathbf{B_1}$ equilibrium does not exist, and iii. a relationship exists between the combined *m* and *n* values and the major product formed.

In addition, it should be mentioned that we were unable to isolate the acetylenic derivatives represented as carbanion $\mathbf{A_1}$ because they evolve towards the allenic form $\mathbf{A_2}$, which is expected to be less stable.

In order to clarify these different points, we carried out an extensive semiempirical study.

Semiempirical MO Study

For this study, we focussed our attention on acetylenic ω-keto esters **1** and **4** which generate a single class of derivative. We considered that three different carbanions (**A**, **B**, and **C**) could be formed in each case, which will be referred to as **1A**–**C** and **4A**–**C**, depending on the starting compound and the type of carbanion formed. In the **A**-type carbanions of compound **4** (cyclohexanone ring), the alkynyl chain may be present in either an equatorial or an axial position,[14] corresponding, respectively, to isomers $\mathbf{4A_{eq}}$ and $\mathbf{4A_{ax}}$ (Scheme 7).

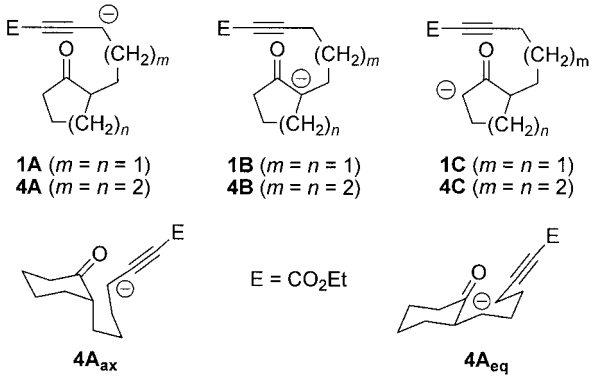

Scheme 7.

In order to obtain energy minima for all the species, we first carried out a systematic conformational analysis employing the AM1 method. Next, the geometries were optimized by performing PM3 calculations. In all cases we invariably found that the **A**-type anions were the most stable. There are two main reasons for this particularly effective stabilization. First, **A**-type carbanions have the most extended charge delocalization. Secondly, the greater the charge delocalization, the greater the number of possible attractive intramolecular interactions with hydrogen atoms. Similarly, the resonant structure of **B**-type carbanions, which has a more substituted C=C double bond, is thermodynamically more stable than the **C**-type anions. The latter are relatively high in energy from a thermodynamic point-of-view and we did not detect any compounds derived from them (i.e. functionalized bridged bicyclic systems). This evidence led us to discard them from this study. In the same way, the axial conformers of **A**-type carbanions are, in general, slightly more stable than the corresponding equatorial conformers. This is essentially due to the fact that an axial disposition of the chain provides a greater number of negative charge–hydrogen-stabilizing interactions (Table 4).

Table 4. AM1- and PM3-calculated relative energies of carbanions **A**, **B**, and **C** for compounds **1** and **4**.[a]

Entry	Anion	AM1 energy [kcal mol^{-1}]	PM3 energy [kcal mol^{-1}]
1	**1A**	0	0
2	**1B**	+5.4	+2.2
3	**1C**	+12.5	+6.2
4	$\mathbf{4A_{ax}}$	0	0
5	$\mathbf{4A_{eq}}$	+2.4	+1.0
6	**4B**	+6.1	+0.6
7	**4C**	+11.4	+11.1

[a] See Scheme 1 within the Supporting Information for a graphical representation of the energies with respect to the reaction coordinate.

Note that carbanions **A** and **B** have very similar energies according to the PM3 calculations. Although **B** anions can be obtained directly by the reaction of TBAF with the starting materials, the most stable conformations of anions **A** and **B** are related by a hydrogen atom that can easily be transferred between the two centres of negative charge. Indeed, it can be seen that these hydrogen atoms are close enough (2.646 and 2.847 Å, respectively) to allow this transfer process (Figure 1).[15]

PM3 calculations show that this hydrogen-transfer process occurs with a low activation energy, as well as there being small energy differences between the **A** and **B** carbanions. This led us to presume that both carbanions are probably involved in a dynamic equilibrium (Scheme 6, Table 5). Conversely, Tables 4 and 5 show that AM1 calculations give particularly high energies for these systems.

Note that hydrogen transfer is much more likely for compound **4**. This means that a six-membered transition state is preferred for this process. In addition, the chain in carbanion **4A** can have either an equatorial or an axial conformation. The results demonstrate, however, that the transfer process in an axial conformation is particularly unstable relative to that in an equatorial position (ca. 3–4.5 kcal mol^{-1}). In fact, in the transition state the system changes to a boat conformation in order to obtain an equatorial position for the chain. Therefore, the chain must be in an equatorial position in the starting carbanion (**4A**) in order to optimize the hydrogen-transfer process (Figure 2). Note also that energy values obtained from AM1 calculations are significantly higher than those obtained by PM3 calculations.[16]

Allenic versus Spiro Pathways

In the formation of allenic derivatives, the diastereoselectivity of the bicycle formation must be considered. Indeed, carbanion **A** could attack the carbonyl carbon atom either on the α-face (*cis* addition) or on the β-face (*trans* addition) (Scheme 8).

Another difference should be highlighted. Formation of the allenic derivative implies a two-step process: 1) formation of the $\mathbf{A_1}$-type carbanion and 2) hydrogen transfer to give the $\mathbf{A_2}$-type carbanion. For the spiro compounds only

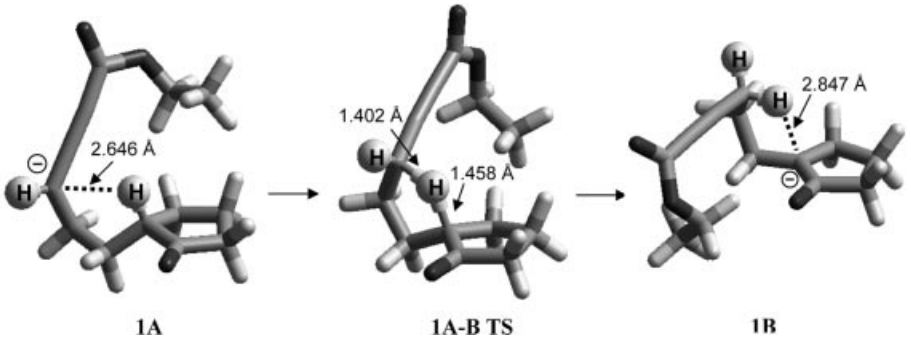

Figure 1. PM3 representations of the most stable conformers of anions **1A** and **1B**, and the transition state for hydrogen transfer (**1A-B TS**) between them.

Table 5. Activation energy for the prototropy between anions **A** and **B**.[a]

Species	Method	Activation energy for the **A** → **B** hydrogen transfer[b] [kcal mol^{-1}]
1A-B TS	AM1	+18.6
	PM3	+8.9
4A$_{eq}$-B TS[c]	AM1	+13.8 (+11.4)
	PM3	+4.8 (+3.8)
4A$_{ax}$-B TS[d]	AM1	+15.8
	PM3	+7.0

[a] See Scheme 1 within the Supporting Information for a graphical representation of the energies with respect to the reaction coordinate. [b] The energies are given relative to those of compounds **1** and **4** (zero energy) in Table 4. [c] Activation energy for the equatorial conformer. The energy values given in brackets are given relative to the energy of **4A$_{eq}$**, the zero reference. [d] Activation energy for the axial conformer. In the transition state, the chain is no longer in an axial position but the system changes to a boat conformation.

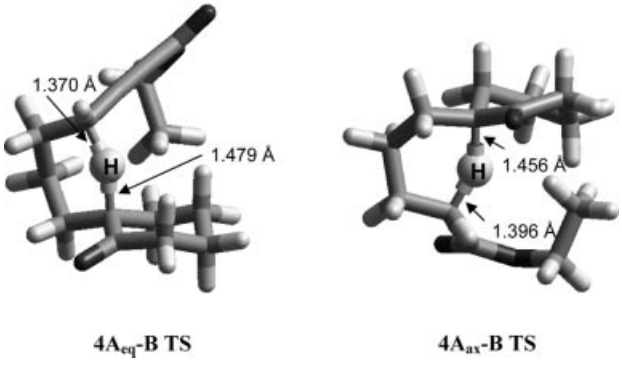

Figure 2. PM3 six-membered transition states for the **4A$_{eq}$** and **4A$_{ax}$** → **4B** hydrogen transfer.

one step is required: the formation of the **B$_1$**-type anion (see Scheme 5).

Compound 1 (n = m = 1)

Table 6 summarizes the energy values of the first step in the synthesis of allenic and spiro derivatives from **1** (formation of **A1** and **B1** carbanions, respectively). In both cases this step corresponds to the generation of a new C–C bond.

From Table 6 the following conclusions can be deduced. First, the allenic derivatives are undoubtedly formed through a *cis* addition process (Entries 2 and 3). This is not surprising since diquinanes are mostly characterized by a *cis* ring junction. The *trans* ring junction leads to highly strained compounds (Figure 3). However, if we take into account the relative energies of **1A** and **1B** (Table 4), the absolute energies of the corresponding transition states (Entries 2 and 9) determined by AM1 calculations are approximately the same. This is a consequence of the large difference in the energies of the parent carbanions (**1A** and **1B**, respectively) found by this semiempirical method and shows that treatment by the AM1 method is inadequate for this particular chemical problem. From PM3 calculations these carbanions have a more similar energy and therefore the spiro pathway is always favored, as found experimentally. Nevertheless, even if the energy difference between both transition states is similar, the rate conversion in each case is considerably different. Thus, at the beginning, molecules have different choices: **1A** can be transformed into **1B**, **1A** can be transformed into **1A$_1$*cis***, **1B** can be transformed back to **1A**, and **1B** can be transformed into **1B$_1$**. Statistically it seems clear that for the majority of the time **1A** is transformed into **1B** and vice versa because they have the most favorable activation energy (8.9 kcal mol^{-1}according to PM3). In fact, **1B** will be converted faster into **1A** because the activation energy for the process **1B** → **1A** is only 6.7 kcal mol^{-1} (Table 4).

Thus, owing to the low energy barrier for the **1A** → **1B** transformation we find at any given moment an appreciable population of **1B** in solution. Moreover, one must remember that **1B** can be formed in solution by direct reaction with TBAF, as we have suggested before, and this is probably the main source of **1B**. Therefore, both species are present in solution and will be transformed independently into **1A$_1$*cis*** or **1B$_1$**, respectively, depending on their corresponding activation energies (Table 6). In addition, the more reactive species in solution (namely the **1B** anion) has the most favorable activation energy (by several kcal mol^{-1}) to proceed along the reaction coordinate. This vision is strongly supported if the reaction occurs under kinetic control, as supported by the experimental data (see Table 1), and also applies to compound 4, which is studied in the next section.

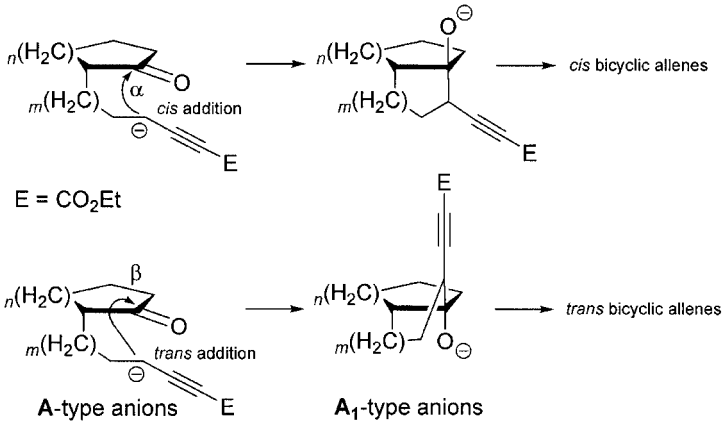

Scheme 8.

Table 6. Energies of the carbanions **1A**, **1A$_1$**, and **1A$_2$** (considering the *cis*/*trans* addition modes), **1B**, **1B$_1$**, and the corresponding transition states. Allenic versus spiro compounds.[a]

Series	Entry	Anion	AM1 energy [kcal mol^{-1}]	PM3 energy [kcal mol^{-1}]
Allenic	1	**1A**	0	0
	2	**1A*cis* TS**	+16.4	+14.6
	3	**1A*trans* TS**	+34.2	+30.9
	4	**1A$_1$*cis***	+13.7	+12.1
	5	**1A$_1$*trans***	+30.6	+28.3
	6	**1A$_2$*cis***	–9.7	–7.1
	7	**1A$_2$*trans***	+8.3	+10.4
Spiro	8	**1B**	0	0
	9	**1B TS**	+11.7	+11.1
	10	**1B$_1$**	–12.5	–15.1

[a] See Scheme 2 within the Supporting Information for a graphical representation of the energies with respect to the reaction coordinate.

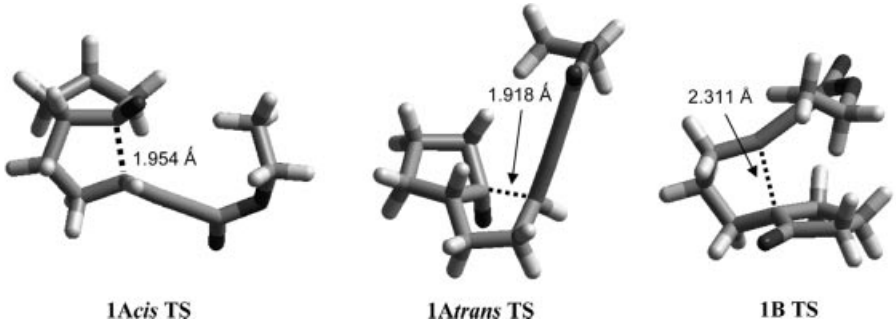

Figure 3. PM3 transition states for the **1A** → **1A$_1$** and **1B** → **1B$_1$** transformations.

Compound 4 (n = m = 2)

The energy values of the first step (C–C bond formation) in the synthesis of allenic and spiro derivatives from **4** are summarized in Table 7.

In contrast to the previous case (*m* = *n* = 1), note that PM3 calculations show that the formation of allenic derivatives is kinetically preferred (ca. 5 kcal mol^{-1}) over that of the spiro compound (Entries 5 and 13). However, the AM1 method gives approximately the same energies for both transition states (**A** → **A$_1$** and **B** → **B$_1$**) (Figure 4). The energy difference between **4A$_1$*trans*$_{eq}$** and **4A$_2$*trans*$_{eq}$** explains why the former compound was never isolated. The reaction always progresses toward allene formation. This significant energy difference can be explained by taking two factors into account: first, the delocalization of the negative charge in the allene system (**4A$_2$*trans*$_{eq}$**) is much more important than the more localized charge in the alkoxide (**4A$_1$*trans*$_{eq}$**) and secondly, the exocyclic allene derivative (sp^2-hybridized carbon) is less strained than the acetylenic side-chain (sp^3-hybridized carbon).[18] Moreover, activation energies indicate that *trans* diastereoselectivity would be expected for decalin skeleton formation (Entries 5 and 4), as found experimentally.

In order to explain the formation of the allenic derivatives it is also necessary to calculate the transition-state energy of the second step, that is, the **4A$_1$*trans*$_{eq}$** → **4A$_2$*trans*$_{eq}$** conversion.

Table 7. Energy values for carbanions **4A**, **4A$_1$**, and **4A$_2$** considering the *cis*/*trans* addition, **4B**, **4B$_1$**, and the corresponding transition states.[16] Allenic vs. spiro compounds.[a]

Series	Entry	Anion	AM1 energy [kcal mol^{-1}]	PM3 energy [kcal mol^{-1}]
Allenic	1	**4A$_{ax}$**	0	0
	2	**4A$_{eq}$**	+2.4	+1.0
	3	**4A*cis*$_{ax}$ TS**	+19.1	+19.3
	4	**4A*cis*$_{eq}$ TS**	+17.4	+18.9
	5	**4A*trans*$_{eq}$ TS**[b]	+14.8	+15.3
	6	**4A$_1$*cis*$_{ax}$**	+15.0	+14.3
	7	**4A$_1$*cis*$_{eq}$**	+12.7	+12.4
	8	**4A$_1$*trans*$_{eq}$**[b]	+10.8	+12.1
	9	**4A$_2$*cis*$_{ax}$**	–8.6	–3.8
	10	**4A$_2$*cis*$_{eq}$**	–11.4	–6.2
	11	**4A$_2$*trans*$_{eq}$**[b]	–12.2	–5.6
Spiro	12	**4B**	0	0
	13	**4B TS**	+14.1	+20.4
	14	**4B$_1$**	–13.3	–13.2

[a] See Scheme 3 within the Supporting Information for a graphical representation of the energies with respect to the reaction coordinate. [b] The *trans*-axial isomer (**4A$_1$*trans*$_{ax}$**) is geometrically impossible.

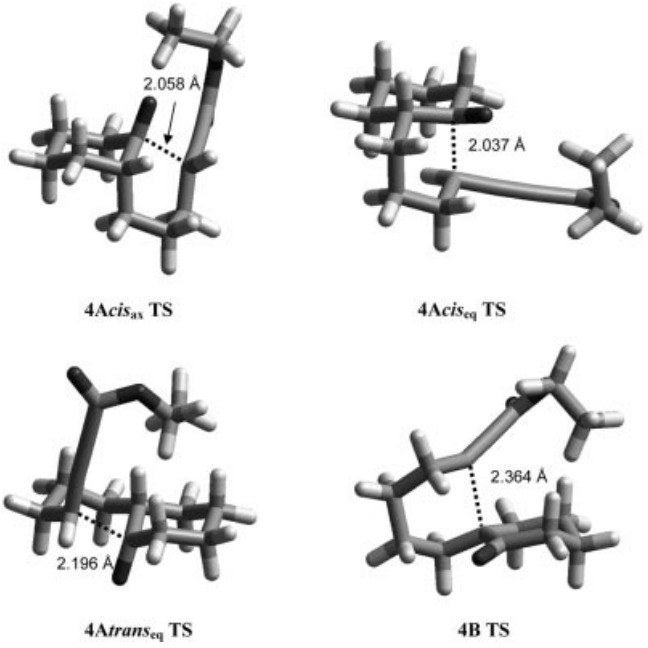

Figure 4. PM3 transition states for the **4A** → **4A$_1$** and **4B** → **4B$_1$** transformations.

The 4A$_1$trans$_{eq}$ → 4A$_2$trans$_{eq}$ Transformation

From the results displayed in Tables 6 and 7 it can be seen that the energy of **A$_1$** lies about 10 kcal mol^{-1} above that of the starting material (**A** carbanion). The "normal" evolution of the **A$_1$** carbanion would be to undergo prototropy to give carbanion **A$_2$**. This process can take place directly by transfer of the chain's base hydrogen to the already formed alkoxide, which implies the formation of a four-membered transition state (**4A$_1$*trans*$_{eq}$ TS**) (Table 8).

Since this transition state connects two atoms with an axial/equatorial relative configuration, a large deformation of the natural angles is found (132° for a sp^3 carbon!), as depicted in Figure 5. This is the main reason for the high activation energies calculated for this process.

Table 8. Energies of the direct **4A$_1$*trans*$_{eq}$** → **4A$_2$*trans*$_{eq}$** hydrogen-transfer process.[a]

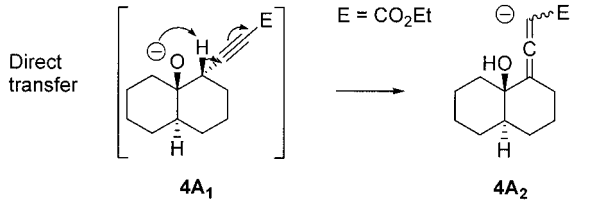

Hydrogen transfer	Anion	AM1 energy [kcal mol^{-1}]	PM3 energy [kcal mol^{-1}]
Direct	**4A$_1$*trans*$_{eq}$**	0	0
	4A$_1$*trans*$_{eq}$ TS	+33.8	+27.0
	4A$_2$*trans*$_{eq}$	–23.0	–17.8

[a] See Scheme 3 within the Supporting Information for a graphical representation of the energies with respect to the reaction coordinate. This direct hydrogen transfer can take place only if there is a *cis* relative configuration between the bridge-head oxo anion and the propargylic hydrogen. This means that the side-chain must be in an axial position.[17]

Therefore, according to these observations, the spiro compounds should once again be the major products, in contrast to the experimental results, which show the formation of only allenic derivatives.

One possible way to achieve this is to diminish the strain energy by avoiding the formation of the four-membered transition state. Thus, it should be noted that the formation of the **A** carbanions induced by TBAF is accompanied by the generation of a hydrogen fluoride (HF) molecule. By studying the role of this species, we have found that, indeed, HF is able to catalyze this hydrogen transfer.

The catalytic effect of the HF molecule can be seen from the data in Table 9. The presence of HF dramatically lowers the activation energy for the hydrogen-transfer process from ca. 27 (Table 8) to ca. 15 kcal mol^{-1}. The proposed mechanism for this process is depicted in Scheme 9.

We suggest that HF can interact with the alkoxide **4A$_1$*trans*$_{eq}$** through the formation of two hydrogen-like

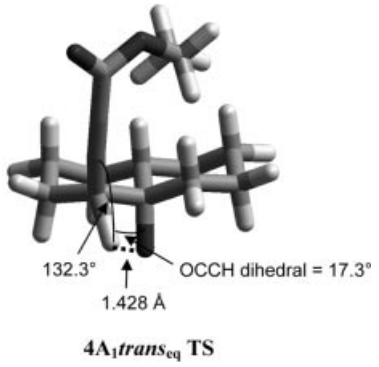

Figure 5. Transition state for direct hydrogen transfer in compound **4**.

Table 9. Energies of the HF-catalyzed $\mathbf{4A_1}$*trans*$_{eq}$ → $\mathbf{4A_2}$*trans*$_{eq}$ hydrogen-transfer process.[a]

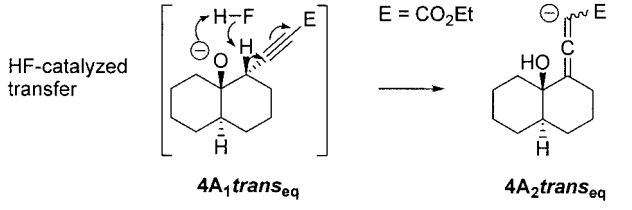

H-Transfer	Anion	PM3 energy [kcal mol^{-1}]
HF-Catalyzed	$\mathbf{4A_1}$*trans*$_{eq}$**-HF**	0
	$\mathbf{4A_1}$*trans*$_{eq}$**-HF TS1**	+15.0
	$E1_{act}$	+15.0
	$\mathbf{4A_1}$*trans*$_{eq}$**-HF inter**	+8.7
	$\mathbf{4A_1}$*trans*$_{eq}$**-HF TS2**	+9.1
	$E2_{act}$	+0.4
	$\mathbf{4A_2}$*trans*$_{eq}$**-HF**	–7.9

[a] See Scheme 4 within the Supporting Information for a graphical representation of the energies with respect to the reaction coordinate. For this case, only the PM3 method can properly treat the presence of the fluorine atom.

bonds. According to PM3 calculations, hydrogen transfer occurs by a two-step mechanism that involves the generation of two six-membered transition states, in contrast to the "direct" transfer in which a four-membered transition state was required. The first step of this mechanism ($\mathbf{4A_1}$*trans*$_{eq}$**-HF** → $\mathbf{4A_1}$*trans*$_{eq}$**-HF inter**) involves the protonation of the alkoxide anion by breaking the HF bond. Then, the generated fluoride anion picks up the propargylic hydrogen atom ($\mathbf{4A_1}$*trans*$_{eq}$**-HF inter** → $\mathbf{4A_2}$*trans*$_{eq}$**-HF**) to finally afford the corresponding allene derivative.

Nevertheless, in order for the **A** → $\mathbf{A_1}$ and **B** → $\mathbf{B_1}$ transformations to have comparable energies, it is necessary to recalculate their energies in the presence of HF. These values are collected in Table 10.

Table 10. Energies of the anions $\mathbf{4A_{ax}}$, $\mathbf{4A_1}$*trans*$_{eq}$, **4B**, $\mathbf{4B_1}$, and the corresponding transition states. Allenic versus spiro compounds in the presence of HF.[a]

Series	Anion	PM3 energy [kcal mol^{-1}]
Allenic	$\mathbf{4A_{ax}}$**-HF**	0
	4A*trans*$_{eq}$**-HF TS**	+16.3
	$\mathbf{4A_1}$*trans*$_{eq}$**-HF**	+5.3
Spiro	**4B-HF**	0
	4B-HF TS	+22.2
	$\mathbf{4B_1}$**-HF**	–12.6

[a] See Schemes 4 and 5 within the Supporting Information for a graphical representation of the energies with respect to the reaction coordinate.

Compound $\mathbf{4A_1}$*trans*$_{eq}$**-HF** lies ca. 5 kcal mol^{-1} above the starting material. This means that the presence of HF greatly stabilizes the intermediate $\mathbf{4A_1}$*trans*$_{eq}$, which was ca. 12 kcal mol^{-1} above **4A** in the absence of HF (Table 7, Entry 8). It has been shown (Table 9) that the activation energy for hydrogen transfer in this intermediate is ca. 15 kcal mol^{-1} (**4A***trans*$_{eq}$**-HF TS**), and therefore this transition state is ca. 20 kcal mol^{-1} above **4A**. This process is the most energy-demanding in the allenic pathway. However,

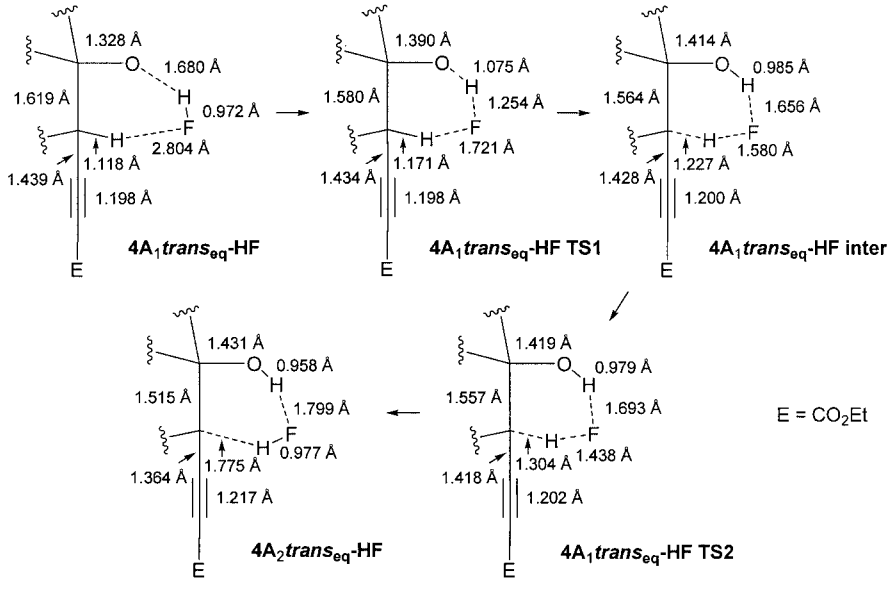

Scheme 9.

the transition state for the **4B-HF** → **4B$_1$-HF** transformation is 22 kcal mol^{-1} above the starting material, showing that the presence of HF favors the allenic pathway, in accord with the experimental results. Of course, 2 kcal mol^{-1} in the correct sense (that is to say, in agreement with the experimental results) is not a big difference in energy, but it is necessary to recognize that in the absence of the HF molecule this value was much higher in the opposite sense. Therefore, we can say that a drastic change in the reaction preference has taken place, and 2 kcal mol^{-1} becomes a significant amount for this particular problem.

Compound 1 (n = m = 1) Revisited

Owing to the large effect of HF on the energies calculated for the transformations of compound **4**, it is also necessary to consider the effect of HF on the transformations of carbanion **1**. In this case, more significant differences were obtained in the presence of HF, as can be seen in Table 11.

Table 11. Energies of the anions **1A**, **1A$_1$*cis***, **1B**, **1B$_1$**, and the corresponding transition states. Allenic versus spiro compounds in the presence of HF.[a]

Series	Anion	PM3 energy [kcal mol^{-1}]
Allenic	**1A-HF**	0
	1A*cis*-HF TS	+12.8
	1A$_1$*cis*-HF	+4.3
	1A$_1$*cis*-HF TS1	+19.4
	$E1_{act}$	+15.1[b]
	1A$_1$*cis*-HF inter	+13.5
	1A$_1$*cis*-HF TS2	+13.8
	$E2_{act}$	+0.2
	1A$_2$*cis*-HF	–6.5
Spiro	**1B-HF**	0[c]
	1B-HF TS	+15.1
	1B$_1$-HF	–18.7

[a] See Schemes 6 and 7 within the Supporting Information for a graphical representation of the energies with respect to the reaction coordinate. [b] The activation energy for the non-HF-catalyzed process (**1A$_1$*cis* TS** species) is 21.4 kcal mol^{-1} (PM3). See Scheme 2 in the Supporting Information. [c] The **1B-HF** structure is only 0.6 kcal mol^{-1} more stable than the **1A-HF** isomer according to the PM3 calculations.

In this case, compound **1A$_1$*cis*-HF** is only ca. 4 kcal mol^{-1} above the starting material, and the hydrogen transfer process in this intermediate has an activation energy of ca. 15 kcal mol^{-1} (therefore the transitions state is ca. 19 kcal mol^{-1} above **1A**). However, for the **1B-HF** → **1B$_1$-HF** transformation, the activation energy is ca. 15 kcal mol^{-1}. Thus, the expected product is the spiro derivative, in accord with the experimental results, and in line with previous calculations (Table 6).

We have analyzed proton transfer in other species. For instance, it is known that commercial TBAF contains a small amount of water. Thus, calculations carried out with water as a catalyst (instead of HF) showed similar behavior, but the activation energies are slightly higher. Other calculations have been carried out involving both water and HF, but the best results were obtained when only HF molecules were considered. Evidently, in solution, there are almost infinite possibilities, but we think that the most probable is the easiest, and once the fluoride anion picks up a hydrogen atom, the HF species then formed remains in the neighborhood of the anion because of strong electrostatic interactions between the anion and the HF molecule. Secondly, the fluoride atom in HF needs to be surrounded by the maximum number of hydrogen atoms in order to be stabilized. It seems normal that a very small molecule like HF, with strong interactions with the molecules under study and in the proximity of the reaction centre, can participate more easily, catalyzing the process. Furthermore, treatment of these molecules with other bases such as NaH, K_2CO_3, NaOEt, *t*BuOK, did not afford any allene derivatives.[3] This probably means that the presence of HF is absolutely necessary.

Conclusions

The synthesis of allenic or spiro derivatives from acetylenic ω-keto esters can be modulated by changing the ring size (*n* value), the chain length (*m* value), or the reaction time. Compounds **1** and **4** have been shown to be suitable starting materials because only one type of product was formed (spiro or allenic derivatives) from them. On the other hand, with regard to the products observed, no evidence for allene–spiro interconversion has been found. Thus, it is clear that the reactions take place under kinetic control. In order to justify the complex behavior of these kinds of products, a semiempirical study was carried out to account for the products formed in each case and the stereochemistry of the bicyclic system generated in the case of the allenic derivatives. In all cases (allenic or spiro), an intramolecular reaction between the frontier orbitals of **A** (for allenic derivatives) or **B** (for spiro compounds) occurs. The activation energy of this process varies as a function of both the size of the cycloalkanone moiety and the chain length. A correct explanation for the whole process can be obtained from PM3 calculations and involves an HF-catalyzed reaction that is very important for compound **4**. In addition, from a qualitative point-of-view, an excellent correlation between the experimental results and the theoretical calculations has been found. For compound **4**, good agreement with the experimental results is found only if we consider that kinetic control (activation energies) governs the reaction.

Experimental Section

General Remarks: Reactions were carried out under argon with magnetic stirring and by using degassed solvents. Et_2O and THF were distilled from Na/benzophenone. Thin-layer chromatography (TLC) was carried out on silica gel plates and the spots were visualized under a UV lamp (254 or 365 nm) and/or sprayed with a solution of vanillin (25 g) in EtOH/H_2SO_4 (98:2; 1 L) or with phosphomolybdic acid followed by heating on a hot plate. For column chromatography, silica gel (40–60 μm) was used. Melting points (m.p.) were measured on a hot stage apparatus. IR spectra were recorded as CCl_4 solutions. ^{1}H NMR spectra were recorded at 200

or 300 MHz and ^{13}C NMR spectra at 50 or 75 MHz using the signal of the residual nondeuteriated solvent as the internal reference. Significant ^1H NMR spectroscopic data are tabulated in the following order: chemical shift (δ) expressed in ppm, multiplicity (s, singlet; d, doublet; t, triplet; q, quadruplet; m, multiplet), coupling constants J in Hertz, number of protons. The ratios of compounds indicated below were calculated from the NMR integrations.

General Procedure for the Treatment of Compounds 1–4 with TBAF: TBAF [1 M solution in THF (1.1 equiv.)] was added to a stirred solution of acetylenic ω-keto esters (1 equiv., 0.4 mmol) in dry THF (5 mL) at room temperature. The yellow solution was stirred at the specified temperature for 30 min, hydrolyzed with a saturated aqueous NH_4Cl solution (10 mL), washed with water (3 × 10 mL), and extracted with Et_2O (2 × 10 mL). The organic layers were then washed with a saturated NaCl solution (10 mL), dried with $MgSO_4$, filtered, and concentrated under reduced pressure (15 Torr, 25 °C). The residue was purified by chromatography on a silica gel column (15 g SiO_2; ethyl acetate/hexane, 1:99 to 15:85) to afford the different products formed.

Compound 1: Colorless oil. IR (CCl_4): $\tilde{\nu}$ = 2240, 1714 cm^{-1}. ^1H NMR (200 MHz, $CDCl_3$, 25 °C): δ = 1.30 (t, J = 7.1 Hz, 3 H), 1.38–188 (m, 8 H), 2.00–2.33 (m, 3 H), 2.34 (t, J = 7.3 Hz, 2 H), 4.22 (q, J = 7.1 Hz, 2 H) ppm. ^{13}C NMR (50 MHz, $CDCl_3$, 25 °C): δ = 14.1, 18.8, 20.8, 25.7, 29.1, 29.7, 38.1, 48.7, 61.8, 73.5, 88.7, 153.8, 220.7 ppm. $C_{13}H_{18}O_3$ (222.28): C 70.24, H 8.16, O 21.59; found C 70.01, H 8.22.

Compound 2: Colorless oil. IR (CCl_4): $\tilde{\nu}$ = 2239, 1742, 1714 cm^{-1}. ^1H NMR (200 MHz, $CDCl_3$, 25 °C): δ = 1.30 (t, J = 7.1 Hz, 3 H), 1.15–2.30 (m, 11 H), 2.34 (t, J = 6.8 Hz, 2 H), 4.21 (q, J = 7.1 Hz, 2 H) ppm. ^{13}C NMR (50 MHz, $CDCl_3$, 25 °C): δ = 13.9, 18.4, 20.7, 26.8, 27.6, 29.3, 29.5, 37.7, 48.5, 61.4, 74.2, 88.6, 153.7, 217.5 ppm. $C_{14}H_{20}O_3$ (236.31): C 71.16, H 8.53, O 21.31; found C 71.17, H 8.66.

Compound 3: Colorless oil. IR (CCl_4): $\tilde{\nu}$ = 2239, 1712 cm^{-1}. ^1H NMR (300 MHz, $CDCl_3$, 25 °C): δ = 1.24 (t, J = 7.1 Hz), 1.25–1.40 (m, 3 H), 1.45–1.70 (m, 6 H), 1.71–1.90 (m, 2 H), 1.91–2.10 (m, 2 H), 2.28 (td, J = 1.5, 7.2 Hz, 2 H), 4.14 (q, J = 7.1 Hz, 2 H) ppm. ^{13}C NMR (75 MHz, $CDCl_3$, 25 °C): δ = 14.1, 18.8, 24.9, 25.3, 27.9, 28.7, 33.9, 40.0, 50.1, 61.6, 73.2, 88.9, 153.7, 212.6 ppm. $C_{14}H_{20}O_3$ (236.31): C 71.16, H 8.53, O 21.31; found C 71.19, H 8.66.

Compound 4: Colorless oil. IR (CCl_4): $\tilde{\nu}$ = 2240, 1714 cm^{-1}. ^1H NMR (300 MHz, $CDCl_3$, 25 °C): δ = 1.27 (t, J = 7.1 Hz), 1.35–2.25 (m, 15 H), 2.32 (t, J = 7.1 Hz), 4.18 (q, J = 7.1 Hz, 2 H) ppm. ^{13}C NMR (75 MHz, $CDCl_3$, 25 °C): δ = 14.0, 18.5, 24.9, 26.4, 27.6, 27.99, 28.7, 33.9, 42.0, 50.5, 61.7, 73.2, 89.1, 153.8, 213.1 ppm. $C_{15}H_{22}O_3$ (250.34): C 71.97, H 8.86, O 19.17; found C 72.03, H 9.00.

Spiro Ketones 5: Spiro ketones **5a** and **5b** (mixture, as a colorless oil) were not separated. IR (mixture **5a** + **5b**, CCl_4): $\tilde{\nu}$ = 1742, 1714, 1652 cm^{-1}. $C_{13}H_{18}O_3$ (222.28) (mixture **5a** + **5b**): C 70.24, H 8.16, O 21.59; found C 70.20, H 8.32.

Spiro Ketone 5a: ^1H NMR (300 MHz, $CDCl_3$, 25 °C): δ = 1.22 (t, J = 7.1 Hz, 3 H), 1.55–2.15 (m, 8 H), 2.20–2.45 (m, 2 H), 2.50–2.60 (m, 1 H), 2.85–3.00 (m, 1 H), 4.03 (qd, J = 2.2, 7.1 Hz, 2 H), 5.50 (t, J = 2.5 Hz) ppm. ^{13}C NMR (75 MHz, $CDCl_3$, 25 °C): δ = 14.2, 19.5, 23.5, 33.5, 36.8, 38.2, 38.3, 59.7, 62.5, 113.0, 166.4, 170.5, 219.6 ppm.

Spiro Ketone 5b: ^1H NMR (300 MHz, $CDCl_3$, 25 °C): δ = 1.18 (t, J = 7.1 Hz, 3 H), 1.55–2.15 (m, 8 H), 2.20–2.45 (m, 2 H), 2.85–3.00 (m, 2 H), 4.10 (q, J = 7.1 Hz, 2 H), 5.85 (t, J = 1.9 Hz, 1 H) ppm. ^{13}C NMR (75 MHz, $CDCl_3$, 25 °C): δ = 14.2, 20.3, 23.2, 36.3, 37.2, 37.4, 39.0, 59.6, 60.9, 112.71, 165.58, 168.82, 219.28 ppm.

Spiro Ketone 5c: Colorless oil. IR (CCl_4): $\tilde{\nu}$ = 1712, 1650 cm^{-1}. ^1H NMR (300 MHz, $CDCl_3$, 25 °C): δ = 1.23 (t, J = 7.1 Hz, 3 H), 1.35–2.15 (m, 7 H), 2.25–2.45 (m, 3 H), 2.94 (ABXYZ, J_{AB} = 15.3, J_{AX} = J_{AY} = J_{AZ} = 1.4, J_{BX} = J_{BY} = J_{BZ} = 2.1 Hz, δ_A = 2.88, δ_B = 3.00, 2 H), 4.09 (q, J = 7.1 Hz, 2 H), 5.88 (m, 1 H) ppm. ^{13}C NMR (75 MHz, $CDCl_3$, 25 °C): δ = 14.1, 19.9, 30.0, 34.2, 34.3, 36.9, 37.4, 61.0, 64.2, 132.9, 136.6, 171.0, 221.0 ppm. $C_{13}H_{18}O_3$ (222.28): C 70.24, H 8.16, O 21.59; found C 70.18, H 8.12.

Compound 6: Colorless oil. IR (CCl_4): $\tilde{\nu}$ = 3500, 2959, 1739, 1652 cm^{-1}. ^1H NMR (300 MHz, $CDCl_3$, 25 °C): δ = 1.23 (t, J = 7.1 Hz, 3 H), 1.72 (q, J = 7.3 Hz, 2 H), 1.78 (quint., J = 7.1 Hz, 2 H), 1.85–2.05 (m, 2 H), 2.13 (t, J = 7.3 Hz, 2 H), 2.29 (t, J = 7.5 Hz, 2 H), 3.04 (s, 1 H), 4.10 (q, J = 7.1 Hz, 2 H) ppm. ^{13}C NMR (75 MHz, $CDCl_3$, 25 °C): δ = 14.1, 22.8, 23.4, 27.6, 33.3, 34.4, 35.4, 36.3, 60.5, 129.1, 138.1, 171.6, 177.0 ppm. $C_{13}H_{20}O_4$ (240.30): C 64.98, H 8.39, O 26.63; found C 65.08, H 8.38.

Spiro Ketone 7a: Colorless oil. IR (CCl_4): $\tilde{\nu}$ = 1739, 1714, 1635 cm^{-1}. ^1H NMR (300 MHz, $CDCl_3$, 25 °C): δ = 1.22 (t, J = 7.1 Hz, 3 H), 1.35–1.95 (m, 8 H), 2.00–2.40 (m, 5 H), 2.66 (dt, J = 9.7, 18.6 Hz, 1 H), 4.06 (ABX_3, J_{AX} = 7.1, J_{BX} = 7.1, J_{AB} = 13.5 Hz, δ_A = 4.09, δ_B = 4.09, 2 H), 5.72 (s, 1 H) ppm. ^{13}C NMR (75 MHz, $CDCl_3$, 25 °C): δ = 14.2, 19.2, 19.6, 23.8, 30.9, 34.2, 34.7, 37.1, 54.8, 59.9, 115.0, 159.1, 166.5, 218.3 ppm. $C_{14}H_{20}O_3$ (236.31): C 71.16, H 8.53, O 20.31; found C 71.22, H 8.42.

Spiro Ketone 7b: Colorless oil. IR (CCl_4): $\tilde{\nu}$ = 1739, 1717, 1635 cm^{-1}. ^1H NMR (300 MHz, $CDCl_3$, 25 °C): δ = 1.17 (t, J = 7.1 Hz, 3 H), 1.30–1.55 (m, 3 H), 1.60–1.90 (m, 6 H), 2.10–2.40 (m, 4 H), 3.51 (dt, J = 4.2, 14.0 Hz, 1 H), 4.04 (qd, J = 2.1, 7.1 Hz, 2 H), 5.34 (s, 1 H) ppm. ^{13}C NMR (75 MHz, $CDCl_3$, 25 °C): δ = 14.1, 18.7, 21.8, 26.2, 27.1, 35.2, 35.7, 38.5, 57.0, 59.6, 113.8, 161.4, 166.3, 219.5 ppm. $C_{14}H_{20}O_3$ (236.31): C 71.16, H 8.53, O 20.31; found C 71.18, H 8.44.

Spiro Ketone 7c: Colorless oil. IR (CCl_4): $\tilde{\nu}$ = 1750, 1648 cm^{-1}. ^1H NMR (300 MHz, $CDCl_3$, 25 °C): δ = 1.25 (t, J = 7.1 Hz, 3 H), 1.50–2.50 (m, 12 H), 2.82 (AB, J_{AB} = 15.1 Hz, δ_A = 2.96, δ_B = 2.68, 2 H), 4.10 (q, J = 7.1 Hz, 2 H), 5.89 (t, J = 3.7 Hz, 1 H) ppm. ^{13}C NMR (75 MHz, $CDCl_3$, 25 °C): δ = 14.2, 19.2, 19.8, 23.8, 30.9, 34.7, 35.0, 37.1, 54.7, 59.9, 115.0, 159.1, 166.5, 218.3 ppm. $C_{14}H_{20}O_3$ (236.31): C 71.16, H 8.53, O 20.31; found C 71.30, H 8.62.

Compound 9: Colorless oil. IR (CCl_4): $\tilde{\nu}$ = 1746, 1682, 1614 cm^{-1}. ^1H NMR (300 MHz, $CDCl_3$, 25 °C): δ = 1.24 (t, J = 7.1 Hz, 3 H), 1.35–1.65 (m, 3 H), 1.70–2.05 (m, 5 H), 2.10–2.40 (m, 3 H), 2.45–2.90 (m, 2 H), 3.54 (AB, J_{AB} = 15.7 Hz, δ_A = 3.57, δ_B = 3.51, 2 H), 4.17 (q, J = 7.1 Hz, 2 H) ppm. ^{13}C NMR (75 MHz, $CDCl_3$, 25 °C): δ = 14.1, 22.0, 23.7, 26.0, 27.2, 32.2, 33.1, 45.1, 47.8, 61.0, 127.1, 162.5, 168.1, 194.3 ppm. $C_{14}H_{20}O_3$ (236.31): C 71.16, H 8.53, O 20.31; found C 71.22, H 8.42.

Allene 10a: Colorless crystals with m.p. 65–66 °C. IR (CCl_4): $\tilde{\nu}$ = 3601, 1964, 1717 cm^{-1}. ^1H NMR (300 MHz, $CDCl_3$, 25 °C): δ = 1.21 (t, J = 7.1 Hz, 3 H), 1.35–1.65 (m, 9 H), 1.80–1.95 (m, 2 H), 2.00–2.15 (m, 1 H), 2.60–2.70 (m, 2 H), 4.11 (ABX_3, J_{AB} = 10.8, J_{BX} = 7.1 Hz, δ_A = 4.07, δ_B = 4.15, 2 H), 5.59 (t, J = 4.1 Hz, 1 H) ppm. ^{13}C NMR (75 MHz, $CDCl_3$, 25 °C): δ = 14.1, 23.1, 24.3, 26.4, 28.0, 28.6, 34.4, 47.3, 60.6, 83.3, 90.8, 112.3, 166.1, 207.0 ppm. $C_{14}H_{20}O_3$ (236.31): C 71.16, H 8.53, O 20.31; found C 71.05, H 8.70.

Allene 10b: Colorless oil. IR (CCl_4): $\tilde{\nu}$ = 3500, 3392, 1963, 1716 cm^{-1}. ^1H NMR (300 MHz, $CDCl_3$, 25 °C): δ = 1.26 (t, J = 7.1 Hz, 3 H), 1.35–1.70 (m, 10 H), 1.80–2.00 (m, 1 H), 2.05–2.25 (m, 1 H), 2.50–2.70 (m, 1 H), 2.71–2.85 (m, 1 H), 4.16 (q, J = 7.1 Hz, 2 H), 5.69 (t, J = 4 Hz, 1 H) ppm. ^{13}C NMR (75 MHz, $CDCl_3$, 25 °C): δ = 14.2, 23.6, 24.0, 26.4, 28.1, 28.3, 34.1, 46.8, 60.8, 83.0, 91.0, 113.6, 166.72, 206.78 ppm. $C_{14}H_{20}O_3$ (236.31): C 71.16, H 8.53, O 20.31; found C 71.32, H 8.69.

Spiro Ketone 11a: Colorless oil. IR (CCl_4): $\tilde{\nu}$ = 1709, 1657 cm^{-1}. ^1H NMR (300 MHz, $CDCl_3$, 25 °C): δ = 1.26 (t, J = 7.1 Hz, 3 H), 1.50–1.90 (m, 8 H), 1.95–2.15 (m, 2 H), 2.25–2.65 (m, 2 H), 2.90 (ddd, J = 2.5, 6.7, 7.7 Hz, 2 H), 4.14 (q, J = 7.3 Hz, 2 H), 5.67 (t, J = 2.5 Hz, 1 H) ppm. ^{13}C NMR (75 MHz, $CDCl_3$, 25 °C): δ = 14.2, 22.1, 22.8, 26.8, 33.0, 37.1, 38.1, 39.1, 59.6, 63.4, 114.3, 166.7, 168.6, 211.0 ppm. $C_{14}H_{20}O_3$ (236.31): C 71.16, H 8.53, O 20.31; found C 71.13, H 8.48.

Spiro Ketone 11b: Colorless oil. IR (CCl_4): $\tilde{\nu}$ = 1709, 1739 cm^{-1}. ^1H NMR (300 MHz, $CDCl_3$, 25 °C): δ = 1.24 (t, J = 7.1 Hz, 3 H), 1.50–2.15 (m, 8 H), 2.20–2.50 (m, 4 H), 3.04 (ABXYZ, $J_{AX} = J_{AY} = J_{AZ}$ = 2.0 Hz, 2 H), 4.12 (q, J = 7.1 Hz, 2 H), 5.77 (dddd, J = 4.4, 1.3, 2.3, 3.6 Hz, 1 H) ppm. ^{13}C NMR (75 MHz, $CDCl_3$, 25 °C): δ = 14.1, 22.1, 26.4, 29.7, 34.3, 35.6, 35.8, 39.6, 60.5, 64.6, 130.3, 138.2, 171.7, 213.2 ppm. $C_{14}H_{20}O_3$ (236.31): C 71.16, H 8.53, O 20.31; found C 71.21, H 8.65.

The spectroscopic data for the allene derivatives **8a**, **8b** and **12a**, **12b** have already been reported.[3a]

Computational Details: The computational study was performed by means of AM1 and PM3 semiempirical MO methods implemented in the Hyperchem™ 7.5 package. Close-shell type calculations (RHF) were carried out, unless otherwise indicated, using the Polak–Ribiere optimization algorithm, except for the transition states for which an eigenvector-following algorithm was employed. Convergence limits for geometry optimization were fixed at 0.01 kcal $Å^{-1}$ mol^{-1} (RMS gradient). The limit for the iterative SCF calculations was fixed at 0.001 kcal mol^{-1}. Transition states were evaluated from estimated initial geometries using a transition-state search implemented in the Hyperchem™ 7.5 package by means of a trial-and-error sequence. This transition state is characterized by its unique negative frequency. Geometries for all the starting carbanions were obtained after a systematic conformational search using the semiempirical methods mentioned above by changing all the dihedral angles in ±30° steps for the acyclic torsion variations. The energies and Cartesian coordinates of all the structures studied are included in the Supporting Information.

Acknowledgments

The authors thank the Junta de Andalucía and the Universidad de Granada for the research contract to A.J.M., and the CNRS and ULP for financial support. We also thank Dr. Jennifer Wytko for her help in preparing the manuscript.

[1] a) L. F. Tietze, U. Beifuss, *Angew. Chem. Int. Ed. Engl.* **1993**, *32*, 131–163; *Angew. Chem.* **1993**, *105*, 137–170; b) L. F. Tietze, *Chem. Rev.* **1996**, *96*, 115–136; c) P. J. Parsons, C. S. Penkett, A. J. Shell, *Chem. Rev.* **1996**, *96*, 195–206; d) A. Padwa, M. D. Weingarten, *Chem. Rev.* **1996**, *96*, 223–269; e) M. Malacria, *Chem. Rev.* **1996**, *96*, 289–306; f) E.-I. Negishi, C. Copéret, S. Ma, S.-Y. Liou, F. Liu, *Chem. Rev.* **1996**, *96*, 365–393; g) K. Neuschütz, J. Velker, R. Neier, *Synthesis* **1998**, 227–255; h) K. C. Nicolaou, D. Vourloumis, N. Winssinger, P. S. Baran, *Angew. Chem. Int. Ed.* **2000**, *39*, 44–122; *Angew. Chem.* **2000**, *112*, 46–126; i) A. J. McCarroll, J. C. Walton, *J. Chem. Soc., Perkin Trans. 1* **2001**, 3215–3229; j) A. J. McCarroll, J. C. Walton, *Angew. Chem. Int. Ed.* **2001**, *40*, 2225–2248; *Angew. Chem.* **2001**, *113*, 2282–2307; k) R. Schobert, G. J. Gordon, *Curr. Org. Chem.* **2002**, *6*, 1181–1196.

[2] M. Miesch, *Synthesis* **2004**, 746–752.

[3] a) F. Wendling, M. Miesch, *Org. Lett.* **2001**, *3*, 2689–2691; b) A. Klein, M. Miesch, *Tetrahedron Lett.* **2003**, *44*, 4483–4485.

[4] a) B. L. Roy, P. Deslongchamps, *Can. J. Chem.* **1986**, *64*, 2068–2075; b) J. F. Lavallée, G. Berthiaume, P. Deslongchamps, *Tetrahedron Lett.* **1986**, *27*, 5455–5458; c) J. F. Lavallée, P. Deslongchamps, *Tetrahedron Lett.* **1987**, *28*, 3457–3458.

[5] J. Christoffers, H. Oertling, *Tetrahedron* **2000**, *56*, 1339–1344.

[6] a) M. Ihara, T. Taniguchi, K. Makita, M. Takano, M. Ohnishi, N. Taniguchi, K. Fukumoto, C. Kabuto, *J. Am. Chem. Soc.* **1993**, *115*, 8107–8115 and references cited therein; b) M. Ihara, K. Fukumoto, *Angew. Chem. Int. Ed. Engl.* **1993**, *32*, 1010–1022; *Angew. Chem.* **1993**, *105*, 1059–1071; c) K. Takasu, M. Ueno, M. Ihara, *J. Org. Chem.* **2001**, *66*, 4667–4672 and references cited therein.

[7] a) P. Chiu, C. P. Szeto, Z. Geng, K. F. Cheng, *Org. Lett.* **2001**, *3*, 1901–1903; b) P. Chiu, B. Chen, K. F. Cheng, *Tetrahedron Lett.* **1998**, *39*, 9229–9232.

[8] a) J. B. Foresman, Æ. Frisch, *Exploring Chemistry with Electronic Structure Methods*, 2nd ed., Gaussian, Inc., Pittsburgh PA, **1996**; b) F. Jensen, *Introduction to Computational Chemistry*, John Wiley & Sons Ltd., Chichester, **1999**.

[9] For examples, see: a) J. W. McIver Jr., A. Komornicki, *J. Am. Chem. Soc.* **1972**, *94*, 2625–2633; b) C. S. Wu, W. C. Neely, S. D. Worley, *J. Comput. Chem.* **1991**, *12*, 862–867; c) Y. L. Dory, P. Soucy, M. Drouin, P. Deslongchamps, *J. Am. Chem. Soc.* **1995**, *117*, 518–529; d) W. M. F. Fabian, G. Kollenz, *J. Chem. Soc., Perkin Trans. 2* **1995**, 515–518; e) A. B. J. Parusel, R. Schamschule, D. Piorun, K. Rechthaler, A. Puchala, D. Rasala, K. Rotkiewicz, G. Köhler, *J. Mol. Struct.* **1997**, *419*, 63–75; f) Z. Markovic, S. Konstantinovic, I. Juranic, L. Dosen-Micovic, *Gazz. Chim. Ital.* **1997**, *127*, 429–434; g) L. Lorenc, V. Pavlovich, I. Juranich, M. L. Mihailovich, L. Bondarenko-Gheorghiu, N. Krstich, M. Dabovich, *Molecules* **1999**, *4*, 272–278; h) M. Grotjahn, N. Jäger, H.-J. Drexler, H.-J. Holdt, E. Kleinpeter, *J. Mol. Model.* **1999**, *5*, 72–77; i) S. Bohm, R. Pohl, J. Kuthan, *Collec. Czech. Chem. Commun.* **1999**, *64*, 1761–1769; j) P. Merino, J. A. Mates, *Arkivoc* **2001**, *xi*, 12–30; k) A. J. Mota, R. Robles, L. Álvarez de Cienfuegos, A. Lamenca, *Tetrahedron Lett.* **2004**, *45*, 3349–3353; l) L. Álvarez de Cienfuegos, A. J. Mota, C. Rodríguez, R. Robles, *Tetrahedron Lett.* **2005**, *46*, 469–473.

[10] A. J. Mota, E. Castellanos, L. Álvarez de Cienfuegos, R. Robles, *Tetrahedron: Asymmetry* **2005**, *16*, 1615–1629.

[11] Hyperchem™, Hypercube, Inc., 1115 NW 4th Street, Gainesville, Florida 32601, USA.

[12] a) H. B. Bürgi, J. D. Dunitz, J.-M. Lehn, G. Wipff, *J. Am. Chem. Soc.* **1974**, *96*, 1956–1957; b) H. B. Bürgi, J. M. Lehn, *Tetrahedron* **1974**, *30*, 1563–1572.

[13] CCDC-271434 (for **10a**), and -271435 (for **12a**) contain the supplementary crystallographic data for this paper. These data can be obtained free of charge from The Cambridge Crystallographic Data Centre via www.ccdc.cam.ac.uk/data_request/cif.

[14] Related to this see: a) K. L. Servis, D. J. Bowler, C. Ishii, *J. Am. Chem. Soc.* **1975**, *97*, 73–80; b) E. A. Basso, C. Kaiser, R. Rittner, J. B. Lambert, *J. Org. Chem.* **1993**, *58*, 7865–7869.

[15] a) B. P. Roberts, *J. Chem. Soc., Perkin Trans. 2* **1996**, 2719–2725; b) M. Ramos, I. Alkorta, J. Elguero, *Tetrahedron* **1997**, *53*, 1403–1410; c) H. F. Dos Santos, L. F. C. De Oliveira, S. O. Dantas, P. S. Santos, W. B. De Almeida, *Int. J. Quantum Chem.* **2000**, *80*, 1076–1086; d) P. E. Allegretti, M. S. Cortizo, C. Guzmán, E. A. Castro, J. J. P. Furlong, *Arkivoc* **2003**, *x*, 24–31; e) C. Öğretir, S. Yarhgan, H. Berber, T. Arslan, S. Topal, *J. Mol. Model.* **2003**, *9*, 390–394.

[16] Higher level DFT (B3LYP/6-31+G*) calculations were carried out for the **1A-B** hydrogen transfer to test both the accuracy of semiempirical calculations and the treatment of anions. We found that this transfer occurs with an activation energy of +15.3 kcal mol^{-1}, compared with values of +18.6 (AM1) and +8.9 kcal mol^{-1} (PM3) found by semiempirical calculations.
[17] The formation of $\mathbf{4A_1}$ derivatives implies the generation of two diastereomers depending on the axial or equatorial position of the electrophilic acetylene side-chain after the cyclisation process. The energies given in Table 7 for these derivatives correspond to the most stable isomer in the transition state. According to PM3 calculations the axial diastereomer is preferred by ca. 2 kcal mol^{-1}, while AM1 calculations showed a preference of only ca. 0.6 kcal mol^{-1} for this conformation.
[18] a) K. B. Wiberg, *Angew. Chem. Int. Ed. Engl.* **1986**, *25*, 312–322; *Angew. Chem.* **1986**, *98*, 312–322; b) T. Dudev, C. Lim, *J. Am. Chem. Soc.* **1998**, *120*, 4450–4458.

Received: May 11, 2005
Published Online: September 1, 2005

